



LNE-SYRTE
GNSS station relative calibration report

G1/G2 #1014-2023

ILNAS
GNSS stations relative calibration.

8 June 2023.
Issue 1.1

Prepared by: Pierre Uhrich, Michel Abgrall, Baptiste Chupin, Caroline Lim

Pierre Uhrich:	+33 1 40 51 22 17	pierre.uhrich@obspm.fr
Michel Abgrall :	+33 1 40 51 20 11	michel.abgrall@obspm.fr
Baptiste Chupin	+33 1 40 51 22 15	baptiste.chupin@obspm.fr

Content

1. Introduction.	3
2. Summary of the results.	4
3. Acronym list and Reference Documents.	5
4.1. Acronym list.	5
4.2. References.	6
4. Description of equipment and operations.	7
4.1. OP GNSS equipment.	7
4.2. UTC(k) GNSS equipment.	7
4.3. Summary of the involved equipment and planning.	7
5. Data and processing.	8
6. Results of data processing.	9
6.1. GPS delays calibration.	9
6.2. Galileo delays calibration.	11
7. Uncertainty budgets.	12
8. Validation of the results.	18
8.1. Stability of the reference station.	18
8.2. Offset between the two traveling receivers.	18
9. Final results for the system to calibrate.	21
9.1. GPS delays.	21
9.2. Galileo delays.	21
9.3. Comparison with former calibrated delays.	22
10. Appendix	23
Annex A. BIPM Information Sheets.	24
Annex B. Raw data and TDEV.	30
Annex C. Uncertainty budget terms.	41
End of Document.	43

1. Introduction.

This calibration report released by LNE-SYRTE is about the G1/G2 relative calibration campaign of GNSS stations located in ILNAS. This campaign took place in ILNAS site from 2 March 2023 (MJD 60005) to 12 March 2023 (MJD 60015).

The report is built according to the Annex 4 of the document “BIPM guidelines for GNSS equipment calibration”, V4.0 05/08/2021 [2], and contains all the required informations, data, plots and results either required by BIPM in the frame of the CCTF Working Group on GNSS, or by BIPM and EURAMET in the frame of the Group1/Group2 calibration scheme. It also contains the uncertainty budget computation according to the Guidelines, which is showing whether the calibrated links used in the frame of the TAI computation would be in line with the conventional values.

This document contains first a summary of the results, followed by a Section devoted to the list of the acronyms used in the document and of the reference documents, Section 4 describes the equipment and operations during the calibration campaign. Section 5 provides all informations about data handling and calibration processing. Section 6 is about the calibration results between stations, and Section 7 is devoted to the uncertainty budgets computation. After an assessment of the stability of the GNSS reference station and of the traveling ones during this campaign in Section 8, the resulting delays and related uncertainties of the calibrated stations are provided in Section 9.

Annex A provides the required BIPM information sheets for all GNSS stations involved, Annex B shows the plots of the raw data together with the related TDEV. Annex C describes all the terms appearing in the uncertainty budgets.

This is Issue 1.1 of this calibration report.

The LNE-SYRTE acknowledges the support of Colleagues in ILNAS.

This report is consistent with the capabilities that are included in Appendix C of the CIPM MRA drawn up by the CIPM. Under the CIPM MRA, all participating institutes recognize the validity of each other's calibration and measurement certificates for the quantities, ranges and measurement uncertainties specified in the KCDB (for details see <https://www.bipm.org/kcdb/>).

2. Summary of the results.

This Section is a summary of the ILNAS GNSS stations relative calibration results. Table 1 provides the GPS P1-code and P2-code calibrated delays for all stations, from where P3 delays are computed, together with their related uncertainties. The deviation from closure having been very small (see Section 7), the combined uncertainties of the GPS P3 delays remain below the 2.5 ns conventional value. As a consequence, Table 1 shows the conventional value from a G1/G2 relative calibration to be considered for all GPS P3 time transfer when using any of the listed stations in the TAI network. These results are fully valid for the period of the calibration campaign.

Table 1. Summary of the UTC(k) stations GPS delays (all values in ns).

Station	Measurement period	P1-code Delays	Combined uncertainty	P2-code Delays	Combined uncertainty	P3 Delays	Combined uncertainty [*]
LU01	60005-60015	28.2	0.7	25.6	0.6	32.2	2.5
LU02	60005-60015	30.6	0.7	28.3	0.6	34.0	2.5

[*] Conventional combined uncertainty value for G1/G2 calibration.

Table 2 provides the Galileo E1-code and E5a-code calibrated delays for all stations, from where E3 delays are computed, together with their related uncertainties. The deviation from closure having been very small (see Section 7), the combined uncertainties of the Galileo E3 delays remain below the 2.5 ns conventional value. As a consequence, Table 2 shows the conventional value from a G1/G2 relative calibration to be considered for all Galileo E3 time transfer when using any of the listed stations in the TAI network. These results are fully valid for the period of the calibration campaign.

Table 2. Summary of the UTC(k) stations Galileo delays (all values in ns).

Station	Measurement period	E1-code Delays	Combined uncertainty	E5a-code Delays	Combined uncertainty	E3 delays	Combined uncertainty [*]
LU01	60005-60015	30.6	0.7	30.8	0.7	30.4	2.5
LU02	60005-60015	32.7	0.7	31.3	0.7	35.0	2.5

[*] Conventional combined uncertainty value for G1/G2 calibration.

3. Acronym list and Reference Document.

3.1. Acronym list:

ADEV :	Allan deviation, square root of AVAR.
AVAR :	Allan variance or two-sample variance.
BIPM:	Bureau International des Poids et Mesures, Sèvres, France.
BRDC :	IGS harmonized GNSS broadcast ephemeris.
CCTF:	Consultative Committee on Time and Frequency.
CGGTTS:	CCTF Global GNSS Time Transfer Standard format.
CIPM:	Comité International des Poids et Mesures.
CV :	Common-View.
DI :	Designated Institute.
EURAMET :	European association of metrology laboratories.
G1:	Group 1 laboratory in the frame of the TAI network.
G2:	Group 2 laboratory in any given Regional Metrology Area.
GLONASS:	Russian GNSS.
GNSS:	Global Navigation Satellite System.
GPS:	United States of America GNSS.
GST:	Galileo System Time.
IGS:	International GNSS Service.
ILNAS:	Institut luxembourgeois de la normalisation, de l'accréditation, de la sécurité et qualité des produits et services, Luxembourg NMI.
LNE:	Laboratoire National de Métrologie et d'Essais, French NMI.
LNE-SYRTE:	French designated laboratory in charge of Time and Frequency units.
MDEV:	Modified Allan deviation, square root of MVAR.
MVAR:	Modified Allan variance.
na:	Not available.
nc:	Not computed.
NMI:	National Metrology Institute.
NRCan :	National Ressources Canada, Canadian NMI.
OP:	Observatoire de Paris, France.
ORB :	Observatoire Royal de Belgique, Brussels, Belgium DI.
PPP :	Precise Point Positioning.
PPS:	Pulse per second.
PTB:	Physikalisch Technische Bundesanstalt, German NMI.
PTF:	Precise Time Facility.
RINEX:	GNSS Receiver International Exchange format for Geodesy.
SYRTE:	Systèmes de Référence Temps-Espace, OP laboratory where LNE-SYRTE is located.
TAI:	Temps Atomique International.
TDEV:	Time Allan deviation, square root of TVAR.
TIC:	Time Interval Counter.
TSP:	Time Service Provider.
TVAR:	Time Allan variance, derived from AVAR and MVAR.
UTC:	Coordinated Universal Time.

3.2. References.

- [1] Pierre Uhrich and David Valat, “*GPS receiver relative calibration campaign preparation for Galileo In-Orbit Validation*”, Proc. of the 24th European Frequency and Time Forum (EFTF), Noordwijk, The Netherlands, April 2010 (CD-Rom).
- [2] BIPM Guidelines for GNSS equipment calibration, v4.0, 05/08/2021.
- [3] G.D. Rovera, J-M. Torre, R. Sherwood, M. Abgrall, C. Courde, M. Laas-Bourez and P. Uhrich, “*Link calibration against receiver calibration: an assessment of GPS time transfer uncertainties*”, Metrologia 51 (2014) 476-490.
- [4] Daniele Rovera, Michel Abgrall, Pierre Uhrich and Marco Siccardi, “*Techniques of antenna cable delay measurement for GPS time transfer*”, Proc. of the 5th International Colloquium on Scientific and Fundamental Aspects of the Galileo Programme, 27-29 October 2015, Braunschweig, Germany.

4. Description of equipment and operations.

4.1. OP GNSS equipment.

The OP GNSS reference station for this campaign is made of one multi-GNSS Septentrio PolaRx5TR main unit called OP73, connected by a 30 m long antenna cable to a SepChoke B3/E6 multi-GNSS antenna. This station was part of the last G1 calibration campaign (#1001-2020), its delays having been computed by BIPM.

The OP GNSS traveling equipment is made of two multi-GNSS Septentrio PolaRx5TR main units called OP72 and OP74, connected to one single 50 m long antenna cable thanks to a power splitter, and to one single multi-GNSS Veraphase VP6000 antenna.

The firmware of all PolaRx5TR was 5.5.0.

4.2. UTC(k) GNSS equipment.

The UTC(k) GNSS equipment to calibrate was based on two Septentrio PolaRx5TR main units. Annex A contains the details about the local implementations in the visited stations.

These stations were calibrated as G2 GNSS stations according to the BIPM Guidelines for the delays computations including the related combined uncertainties. But the resulting uncertainties will also be provided within the 95 % uncertainty level as recommended by EURAMET.

4.3. Summary of the involved equipment and planning.

Table 3 summarizes the equipment involved in the GNSS relative calibration campaign of UTC(k) laboratories with highlighted traveling station measurement periods on each site.

Table 3. Summary of equipment and planning.

Institute	Equipment status	MJD of measurement	Receiver type	BIPM code	RINEX name
OP	Traveling	59986 - 60030	Septentrio PolaRx5TR	OP72	OP72
OP	Traveling	59986 - 60030	Septentrio PolaRx5TR	OP74	OP74
OP	G1 reference	59986 - 60030	Septentrio PolaRx5TR	OP73	OP7300FRA
LU01	G2	60005-60015	Septentrio PolaRx5TR	LU01	LU0100LUX
LU02	G2	60005-60015	Septentrio PolaRx5TR	LU02	LU0200LUX

5. Data and processing.

All OP collected raw Septentrio binary files (SBF) data are transformed into GNSS RINEX 3 format by using the Septentrio proprietary SBF2RIN software. Local receivers SBF and/or RINEX 3 and/or RINEX 2 data, together with CGGTTS files when they exist, are provided by the visited institution/laboratory. The calibration is consisting in building differential 30 s sampled CGGTTS data for each P1- and P2-codes for GPS and for each E1- and E5a-codes for Galileo between pairs of receivers, for which we partly use the R2CGGTTS software developed by P. Defraigne (ORB). Another part of the calibration software is an original development by LNE-SYRTE. These CGGTTS differences are corrected by the known reference delay (REFDLY) and antenna cable delay (CABDLY) when available. In this case, the calibrated delays are for the ensemble receiver main unit plus antenna.

For each location, the coordinates of the antenna phase centers are especially computed for the calibration period from RINEX files by using the NRCAN PPP software. Unfortunately, this computation is limited to GPS phase center for L1 and L2 carrier frequencies. Galileo E1 carrier being equal to L1, we assume the phase center is identical. But it is not the case for Galileo E5a compared to L2, and we can only approximate the Galileo E5a phase center by using L2 one. The geometric correction between pairs of antenna phase centers for receivers in common-clock set-up is computed by using Rapid BRDC files provided by IGS.

Reference delays are measured against either the local UTC(k) physical reference point or the local time scale reference point at the trigger level currently used in the involved laboratories. The trigger level in LNE-SYRTE is 1.0 V. Antenna cable delay is either obtained from dedicated measurements or included in the P1 and P2 delays and in the E1 and E5a delays when no value is available for this parameter. In this latter case, the CABDLY value is set to 0 in the parameter file, and the calibrated delays are for the ensemble receiver main unit plus antenna cable plus antenna.

For validation purposes, ionosphere-free linear combinations P3 and E3 CGGTTS files are computed by using the R2CGGTTS software provided by P. Defraigne (ORB), and CV are built between pairs of receivers. This is more especially the case when we are using two traveling receivers in a visited location, in order to better assess the stability of this traveling ensemble all over the calibration campaign. But this usual validation process cannot be applied when both traveling receivers are not connected to the same local time scale. The conservative estimated value for the traveling equipment stability during such a campaign is typically chosen for each code as the maximum between the misclosure between the start and the end of the campaign and the average offset between both traveling receivers as measured in each location.

As conservative estimate, the noise of the P1 and P2 differences and of the E1 and E5a differences is obtained from the highest value of the one-sigma statistical uncertainty of the TDEV at 1 d, issued from a linear interpolation between consecutive TDEV points when required. In the case there is not enough data to compute a TDEV at 1 d, the upper limit of the last error bar available is considered as noise of the raw differences. The noise of P3 and E3 data is issued from a similar analysis on TDEV data.

6. Results of data processing.

6.1. GPS delays calibration.

The plots of the GPS codes raw data processing and the related TDEV can be found in Annex B. Table 4 to 6 provide a summary of all the delays involved in the GPS code calibrations for all stations. First, the calibration of the traveling stations OP72 and OP74 against the reference station OP73, leading to the OP72 and OP74 delay mean values between the start and the end of the campaign. Second, the calibration of the visited stations against these mean values. As typically expected, the noise estimates from the TDEVs are below 100 ps, and are hence remaining low enough in the uncertainty budgets (see Section 7).

*Table 4. Summary of GPS delays for traveling stations **OP72 and OP74** (all values in ns).*

Receiver	Reference	MJD of Measurement	REFDLY	CABDLY	P1 DLY	TDEV	P2 DLY	TDEV
OP73	1001-2020	59986 – 59991	85.2	129.6	29.500	NC	26.300	NC
OP72	OP73	59986 – 59991	93.4	0.0	224.535	0.027	222.625	0.030
OP74	OP73	59986 – 59991	111.4	0.0	225.204	0.021	223.385	0.024
OP73	1001-2020	60025-60030	85.2	129.6	29.500	NC	26.300	NC
OP72	OP73	60025-60030	93.3	0.0	224.313	0.031	222.576	0.027
OP74	OP73	60025-60030	111.4	0.0	225.046	0.031	223.369	0.026

*Table 5. Summary of GPS delays for visited stations against **OP72 mean delays** (all values in ns).*

Receiver	Reference	MJD of Measurement	REFDLY	CABDLY	P1 DLY	TDEV	P2 DLY	TDEV
OP72	OP73	60005-60015	50.2	0.0	224.424	NC	222.600	NC
LU01	OP72	60005-60015	36.6	117.4	28.172	0.091	25.580	0.051
LU02	OP72	60005-60015	38.6	160.6	30.504	0.090	28.256	0.049

*Table 6. Summary of GPS delays for visited stations against **OP74 mean delays** (all values in ns).*

Receiver	Reference	MJD of Measurement	REFDLY	CABDLY	P1 DLY	TDEV	P2 DLY	TDEV
OP74	OP73	60005-60015	68.2	0.0	225.125	NC	223.377	NC
LU01	OP74	60005-60015	36.6	117.4	28.267	0.090	25.694	0.051
LU02	OP74	60005-60015	38.6	160.6	30.600	0.091	28.369	0.050

Table 7 provides the differential GPS delays of the visited systems with respect to the traveling system, according to BIPM Guidelines [2]. We note here that the offsets of the differences between either OP72 or OP74 and OP73 at the start and at the end of the campaign are about -0.222 ns (P1) and -0.049 ns (P2) for OP72 and -0.158 ns (P1) and -0.016 ns (P2) for OP74 respectively, which is small enough to provide excellent resulting uncertainty budgets (see Section 7). In addition, there is also a very good consistency of the remote station delays obtained either from OP72 or from OP74 in each visited location, the maximum offset between both staying below 114 ps.

Table 7. Visited systems with respect to reference system via traveling systems (all values in ns).

Pair	MJD of Measurement	INTDLY P1	INTDLY P2	P1 – P2
OP72 – OP73	59986 – 59991	224.535	222.625	1.910
OP74 – OP73	59986 – 59991	225.204	223.385	1.819
OP72 – OP73	60025-60030	224.313	222.576	1.737
OP74 – OP73	60025-60030	225.046	223.369	1.677
LU01– OP72	60005-60015	28.172	25.580	2.592
LU01– OP74	60005-60015	30.504	28.256	2.248
LU02 – OP72	60005-60015	28.267	25.694	2.573
LU02 – OP74	60005-60015	30.600	28.369	2.231

6.2. Galileo delays calibration.

The plots of the Galileo codes raw data processing and related TDEV can be found in Annex B. Table 8 to 10 provide a summary of all the delays involved in the Galileo code calibrations for all stations. First, the calibration of the traveling stations OP72 and OP74 against the reference station OP73, leading to the OP72 and OP74 delay mean values between the start and the end of the campaign. Second, the calibration of the visited stations against these mean values. As typically expected, the noise estimates from the TDEVs are about or below 100 ps, and are hence remaining low enough in the uncertainty budgets (see Section 7).

Table 8. Summary of Galileo delays for traveling stations OP72 and OP74 (all values in ns).

Receiver	Reference	MJD of Measurement	REFDLY	CABDLY	E1 DLY	TDEV	E5a DLY	TDEV
OP73	1001-2020	59986 – 59991	85.2	129.6	31.700	NC	31.300	NC
OP72	OP73	59986 – 59991	93.4	0.0	226.840	0.038	226.055	0.056
OP74	OP73	59986 – 59991	111.4	0.0	227.649	0.034	226.801	0.043
OP73	1001-2020	60025-60030	85.2	129.6	31.700	NC	31.300	NC
OP72	OP73	60025-60030	93.3	0.0	226.598	0.046	225.985	0.045
OP74	OP73	60025-60030	111.4	0.0	227.476	0.048	226.761	0.046

Table 9. Summary of Galileo delays for all visited stations against OP72 mean delays (all values in ns).

Receiver	Reference	MJD of Measurement	REFDLY	CABDLY	E1 DLY	TDEV	E5a DLY	TDEV
OP72	OP73	60005-60015	50.2	0.0	226.719	NC	226.020	NC
LU01	OP72	60005-60015	36.6	117.4	30.592	0.092	30.753	0.059
LU02	OP72	60005-60015	38.6	160.6	32.681	0.104	31.268	0.060

*Table 10. Summary of Galileo delays for all visited stations against **OP74** mean delays (all values in ns).*

Receiver	Reference	MJD of Measurement	REFDLY	CABDLY	E1 DLY	TDEV	E5a DLY	TDEV
OP74	OP73	60005-60015	68.2	0.0	227.563	NC	226.781	NC
LU01	OP74	60005-60015	36.6	117.4	30.686	0.091	30.867	0.063
LU02	OP74	60005-60015	38.6	160.6	32.775	0.103	31.381	0.060

Table 11 provides the differential Galileo delays of the visited systems with respect to the traveling system, according to BIPM Guidelines [2]. We note here that the offsets of the differences between either OP72 or OP74 and OP73 at the start and at the end of the campaign are about $-0,242$ ns (E1) and $-0,070$ ns (E5a) for OP72 or $-0,173$ ns (E1) and $-0,040$ ns (E5a) for OP74, which is small enough to provide excellent resulting uncertainty budgets (see Section 7). In addition, there is also a very good consistency of the remote station delays obtained either from OP72 or from OP74 in each visited location, the maximum offset between both staying below 114 ps.

Table 11. Visited systems with respect to reference system via traveling system (all values in ns).

Pair	MJD of Measurement	INTDLY E1	INTDLY E5a	E1 – E5a
OP72 – OP73	59986 – 59991	226.840	226.055	0.785
OP74 – OP73	59986 – 59991	227.649	226.801	0.848
OP72 – OP73	60025-60030	226.598	225.985	0.613
OP74 – OP73	60025-60030	227.476	226.761	0.715
LU01 – OP72	60005-60015	30.592	30.753	- 0.161
LU01 – OP74	60005-60015	32.681	31.268	1.413
LU02 – OP72	60005-60015	30.686	30.687	- 0.181
LU02 – OP74	60005-60015	32.775	31.381	1.394

7. Uncertainty budgets.

We provide in this section an estimation of the combined uncertainty of the differential calibration for the receivers located in visited laboratories. All the uncertainty budgets have been built according to the reference [2] in order to provide the required u_{CAL0} values. More details on the uncertainty estimations are provided in Annex C.

The Type A uncertainty on measured codes is estimated from the high value of the 1 sigma statistical uncertainty of the TDEV(1 d). The Type A uncertainty of the difference between codes is the quadratic sum between both estimations. But the P3 and E3 Type A uncertainties are estimated from the high value of the 1 sigma statistical uncertainty of the related TDEV(1 d). All TDEV plots are in Annex B. Table 12 shows the P3 and E3 TDEV(1 d) computed values for all receiver pairs during the campaign. Note how OP72 and OP74 P3 and E3 noises are staying close to each other at the start and at the end of the campaign at OP. This is mostly because they are connected to the same antenna cable and antenna. The conservative values eventually chosen for the uncertainty budget computation are highlighted in **bold purple**.

Table 12. One sigma statistical uncertainty computed values of TDEV(1 d) for P3 and E3 for all station pairs (all values in ns).

Linear combination	P3	E3
OP72 – OP73 Start	0.070	0.051
OP72 – OP73 End	0.100	0.093
OP74 – OP73 Start	0.072	0.055
OP74 – OP73 End	0.097	0.094
LU01 – OP72	0.279	0.199
LU01 – OP74	0.278	0.195
LU02 – OP72	0.294	0.216
LU02 – OP74	0.294	0.214

In the calibration process only P1 and P2 delays for GPS and E1 and E5a delays for Galileo are estimated, therefore the misclosure for P3 delay (GPS) or E3 delay (Galileo) is not directly available from the calibration computation. The GPS P3 misclosure is estimated by applying to the misclosure values computed for P1- and P2-code the ionosphere-free linear combination formula:

$$P3 = P1 + 1.546 \times (P1 - P2)$$

The Galileo E3 misclosure is estimated by applying to the misclosure values computed for E1- and E5a-code the ionosphere-free linear combination formula:

$$E3 = E1 + 1.261 \times (E1 - E5a)$$

Table 13 shows the values of the considered misclosures. All these results are excellent and even close to the state of the art, leading to uncertainty budgets which will be in the lowest part of such computation. Note that only positive offsets will be used as u_b values in the uncertainty budget computation.

Table 13. Mean values of deviation from closure between traveling stations and reference station OP73 (all values in ns).

<i>Misclosure</i>	$\Delta P1$	$\Delta P2$	$\Delta(P1 - P2)$	$\Delta P3$	$\Delta E1$	$\Delta E5a$	$\Delta(E1 - E5a)$	$\Delta E3$
OP72	- 0.222	- 0.049	- 0.173	- 0.489	- 0.242	- 0.070	- 0.172	- 0.459
OP74	- 0.158	- 0.016	- 0.142	- 0.378	- 0.173	- 0.040	- 0.133	- 0,341
Mean value	- 0.190	- 0.033	- 0.158	- 0.434	- 0.208	- 0.055	- 0.153	- 0.400

Table 14 and 15 are providing the uncertainty budgets for GPS delays of all visited stations. Table 16 and 17 are providing similar uncertainty budgets for Galileo delays of all visited stations tracking Galileo signal.

Table 14. LU01 uncertainty budget for GPS calibrated delays (all values in ns).

Uncertainty type	P1	P2	P1 – P2	P3	Description
u _a (reference)	0.031	0.030	0.043	0.100	Largest TDEV(1 d) sigma between the start and the end of OP72 or OP74 against OP73
u _a (LU01)	0.091	0.051	0.104	0.279	Largest TDEV(1 d) sigma of offset between visited station and OP72 or OP74
Type A uncertainties					
u _a	0.096	0.059	0.113	0.296	Visited against reference
Misclosure					
u _{b,1}	0.190	0.033	0.158	0.434	Actual misclosure offset
Systematic components related to RAWDIF					
u _{b,11}	0.200	0.200	0.200	0.200	Position error at OP
u _{b,12}	0.200	0.200	0.200	0.200	Position error at visited site
u _{b,13}	0.200	0.200	0.200	0.200	Multipaths at OP
u _{b,14}	0.200	0.200	0.200	0.200	Multipaths at visited site
Link of the traveling system to local time scales					
u _{b,21}	0.220	0.220		0.220	REFDLY at OP
u _{b,22}	0.220	0.220		0.220	REFDLY at visited site
u _{b,TOT}	0.541	0.508	0.430	0.667	
Link of the reference system to UTC(OP)					
u _{b,31}	0.220	0.220		0.220	REFDLY at OP
Link of the visited system to its local time scale					
u _{b,32}	0.220	0.220		0.220	REFDLY at visited site
Antenna cable delays					
u _{b,41}	0.0	0.0		0.0	CABDLY at OP
u _{b,42}	0.0	0.0		0.0	CABDLY at visited site
Type B uncertainties					
u _{b,SYS}	0.624	0.596		0.736	Quadratic sum of u _b
Combined uncertainties					
u _{CAL0}	0.631	0.599		0.793	Composed of u _a and u _{b,SYS}

Table 15. LU02 uncertainty budget for GPS calibrated delays (all values in ns).

Uncertainty type	P1	P2	P1 – P2	P3	Description
u_a (reference)	0.031	0.030	0.043	0.100	Largest TDEV(1 d) sigma between the start and the end of OP72 or OP74 against OP73
u_a (LU02)	0.091	0.050	0.104	0.294	Largest TDEV(1 d) sigma of offset between visited station and OP72 or OP74
Type A uncertainties					
u_a	0.096	0.058	0.113	0.311	Visited against reference
Misclosure					
$u_{b,1}$	0.190	0.033	0.158	0.434	Actual misclosure offset
Systematic components related to RAWDIF					
$u_{b,11}$	0.200	0.200	0.200	0.200	Position error at OP
$u_{b,12}$	0.200	0.200	0.200	0.200	Position error at visited site
$u_{b,13}$	0.200	0.200	0.200	0.200	Multipaths at OP
$u_{b,14}$	0.200	0.200	0.200	0.200	Multipaths at visited site
Link of the traveling system to local time scales					
$u_{b,21}$	0.220	0.220		0.220	REFDLY at OP
$u_{b,22}$	0.220	0.220		0.220	REFDLY at visited site
$u_{b,TOT}$	0.541	0.508	0.430	0.667	
Link of the reference system to UTC(OP)					
$u_{b,31}$	0.220	0.220		0.220	REFDLY at OP
Link of the visited system to its local time scale					
$u_{b,32}$	0.220	0.220		0.220	REFDLY at visited site
Antenna cable delays					
$u_{b,41}$	0.0	0.0		0.0	CABDLY at OP
$u_{b,42}$	0.0	0.0		0.0	CABDLY at visited site
Type B uncertainties					
$u_{b,SYS}$	0.624	0.596		0.736	Quadratic sum of u_b
Combined uncertainties					
u_{CAL0}	0.631	0.599		0.799	Composed of u_a and $u_{b,SYS}$

Table 16. LU01 uncertainty budget for Galileo calibrated delays (all values in ns).

Uncertainty type	E1	E5a	E1 – E5a	E3	Description
u_a (Reference)	0.048	0.057	0.075	0.094	Largest TDEV(1 d) sigma between the start and the end of OP72 or OP74 against OP73
u_a (LU01)	0.092	0.063	0.112	0.199	Largest TDEV(1 d) sigma of offset between visited station and OP72 or OP74
Type A uncertainties					
u_a	0.104	0.085	0.135	0.220	Visited against reference
Misclosure					
$u_{b,1}$	0.208	0.055	0.153	0.400	Actual misclosure offset
Systematic components related to RAWDIF					
$u_{b,11}$	0.200	0.200	0.200	0.200	Position error at OP
$u_{b,12}$	0.200	0.200	0.200	0.200	Position error at visited site
$u_{b,13}$	0.200	0.200	0.200	0.200	Multipaths at OP
$u_{b,14}$	0.200	0.200	0.200	0.200	Multipaths at visited site
Link of the traveling system to local time scales					
$u_{b,21}$	0.220	0.220		0.220	REFDLY at OP
$u_{b,22}$	0.220	0.220		0.220	REFDLY at visited site
$u_{b,TOT}$	0.517	0.510	0.347	0.552	
Link of the reference system to UTC(OP)					
$u_{b,31}$	0.220	0.220		0.220	REFDLY at OP
Link of the visited system to its local time scale					
$u_{b,32}$	0.220	0.220		0.220	REFDLY at visited site
Antenna cable delays					
$u_{b,41}$	0.0	0.0		0.0	CABDLY at OP
$u_{b,42}$	0.0	0.0		0.0	CABDLY at visited site
Type B uncertainties					
$u_{b,SYS}$	0.603	0.597		0.634	Quadratic sum of u_b
Combined uncertainties					
u_{CAL0}	0.612	0.603		0.671	Composed of u_a and $u_{b,SYS}$

Table 17. LU02 uncertainty budget for Galileo calibrated delays (all values in ns).

Uncertainty type	E1	E5a	E1 – E5a	E3	Description
u_a (Reference)	0.048	0.057	0.075	0.094	Largest TDEV(1 d) sigma between the start and the end of OP72 or OP74 against OP73
u_a (LU02)	0.104	0.060	0.120	0.216	Largest TDEV(1 d) sigma of offset between visited station and OP72 or OP74
Type A uncertainties					
u_a	0.115	0.083	0.142	0.236	Visited against reference
Misclosure					
$u_{b,1}$	0.208	0.055	0.153	0.400	Actual misclosure offset
Systematic components related to RAWDIF					
$u_{b,11}$	0.200	0.200	0.200	0.200	Position error at OP
$u_{b,12}$	0.200	0.200	0.200	0.200	Position error at visited site
$u_{b,13}$	0.200	0.200	0.200	0.200	Multipaths at OP
$u_{b,14}$	0.200	0.200	0.200	0.200	Multipaths at visited site
Link of the traveling system to local time scales					
$u_{b,21}$	0.220	0.220		0.220	REFDLY at OP
$u_{b,22}$	0.220	0.220		0.220	REFDLY at visited site
$u_{b,TOT}$	0.517	0.510	0.347	0.552	
Link of the reference system to UTC(OP)					
$u_{b,31}$	0.220	0.220		0.220	REFDLY at OP
Link of the visited system to its local time scale					
$u_{b,32}$	0.220	0.220		0.220	REFDLY at visited site
Antenna cable delays					
$u_{b,41}$	0.0	0.0		0.0	CABDLY at OP
$u_{b,42}$	0.0	0.0		0.0	CABDLY at visited site
Type B uncertainties					
$u_{b,SYS}$	0.603	0.597		0.634	Quadratic sum of u_b
Combined uncertainties					
u_{CAL0}	0.614	0.603		0.676	Composed of u_a and $u_{b,SYS}$

8. Validation of the results.

8.1. Stability of the reference station.

The reference station in OP was based on a Septentrio PolaRx5TR receiver called OP73. Figure 2 is showing a plot which demonstrate the stability of this GNSS station during the calibration campaign. The plot is the daily averaged offset between the Two-Way Satellite Time and Frequency Transfer (TWSTFT) between OP and PTB, based on the Software-Defined Radio (SDR) technique, and the GNSS Common View (CV) time transfer using P3 GPS data between OP and PTB, based on OP73 in OP side and on PTBB in PTB side. In both laboratories, the signal source is a UTC(k) time scale: UTC(PTB) and UTC(OP). In this computation, the time scales being cancelled, what remains is only the offset between the two time transfer techniques.

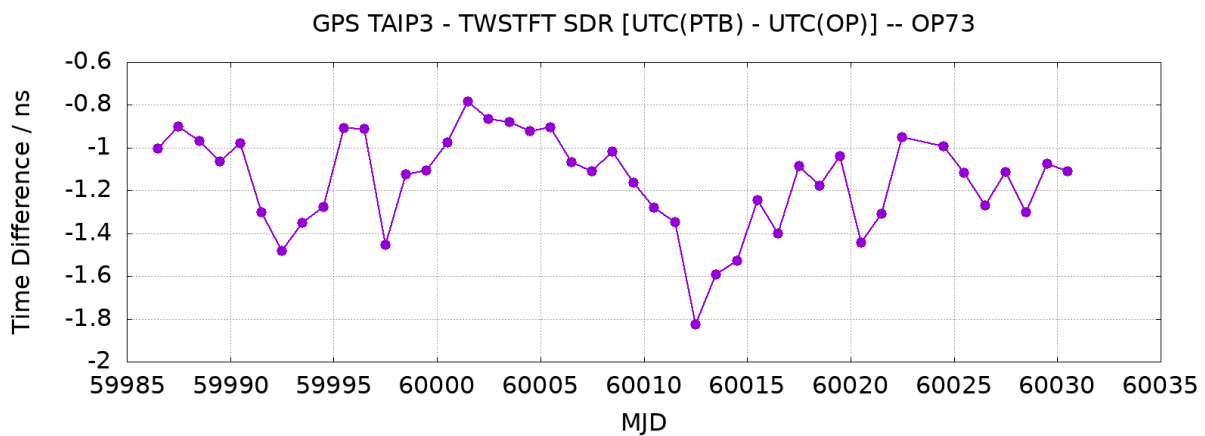


Figure 2. Daily averaged offset between TWSTFT and GPS P3 CV on the link OP-PTB during the calibration campaign.

The mean offset over that period of time is about $-1,01$ ns, with a standard deviation of about $0,22$ ns. This mean offset is mostly coming from the last G1 calibration of GNSS stations achieved by BIPM for OP and PTB stations (#1001-2020) and from the last TWSTFT relative calibration (#0546-2021). We remind here that the conventional combined uncertainty of GNSS stations located in G1 laboratories is $1,5$ ns, as decided by the CCTF Working Group (WG) on GNSS time transfer. The offset seen here is in full agreement with the claimed uncertainties.

What can be seen on Figure 2 is the excellent sub-ns stability of this ensemble of four systems, two inside each laboratory, among which OP73 in OP. This is especially true when considering together the opening and closing periods of the campaign only, MJD 59986-59991 and MJD 60025-60030. We estimate that any potential effect of OP73 on this calibration campaign can be disregarded with respect to the final uncertainty of the calibration (see Section 9).

8.2. Offset between the two traveling receivers.

Figure 3 is showing the offset between the two traveling receivers during the whole calibration campaign, based on CV between CGGTTS P3 (GPS), and Figure 4 is showing similar offset based on CV between CGGTTS E3 (Galileo) data, by using for OP72 and OP74 the average delays computed against OP73 between the start and the closure of the campaign.

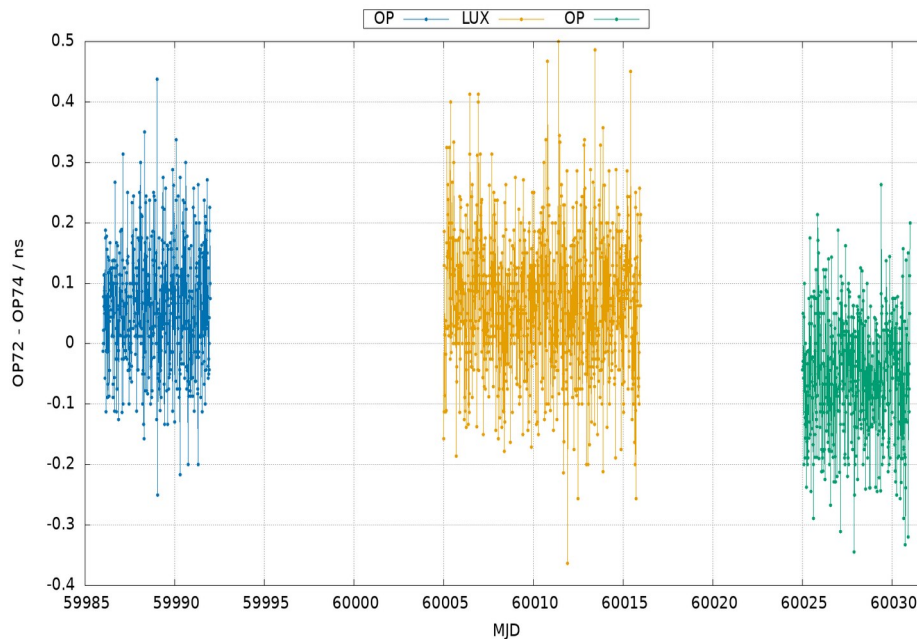


Figure 3. Offset between OP72 and OP74 during the UTC(k) calibration campaign, based on CGGTTS P3 CV data. From left to right, the sequence of data sets is: start at OP, ILNAS and closure at OP.

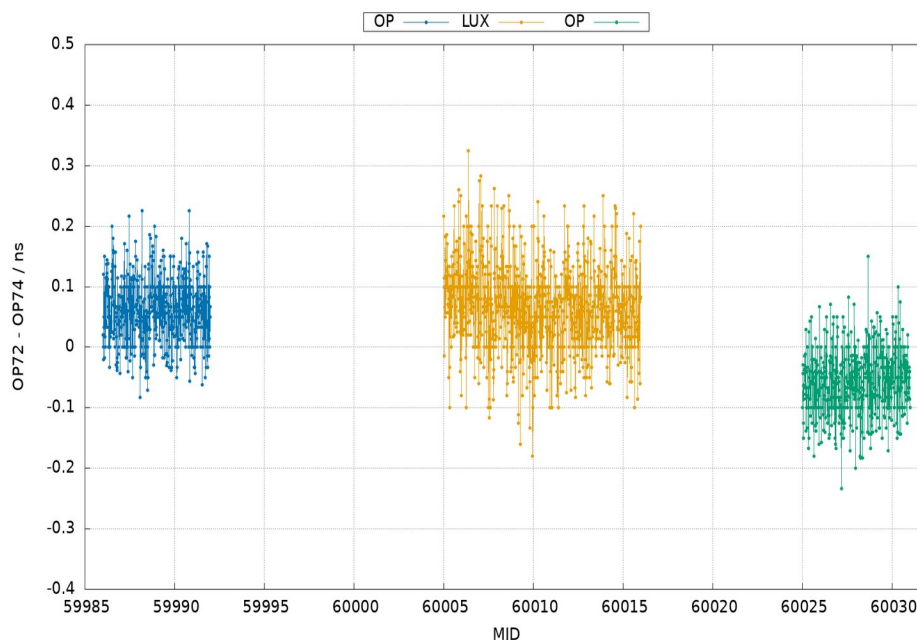


Figure 4. Offset between OP72 and OP74 during the UTC(k) calibration campaign, based on CGGTTS E3 CV data. From left to right, the sequence of data sets is: start at OP, ILNAS and closure at OP.

Table 18 provides the mean values and standard deviations for all periods and data related to the plots above. What can be seen here is a clear consistency largely below 100 ps between both traveling receivers all over the campaign. We also see here that, even if the mean offsets are staying very close, all the GPS CV are appearing significantly more noisy than the related Galileo CV, noting that the main units are connected to one single antenna and one single antenna cable.

Table 18. Offsets between OP72 and OP74 during the ILNAS calibration campaign (all values in ns).

OP72 - OP74	GPS CV mean value	Standard deviation	Galileo CV mean value	Standard deviation
OP (start)	0.059	0.099	0.061	0.055
ILNAS	0.067	0.111	0.067	0.070
OP (closure)	- 0.057	0.099	- 0.058	0.053

9. Final results for the systems to calibrate.

In this Section, we provide the final results of the calibration campaign, based on the uncertainty budgets of Section 8, and according to the BIPM guidelines [2]. In addition, we also provide a conservative $k = 2$ computation of the uncertainties (95 % confidence interval), according to the EURAMET recommendations. All visited stations are calibrated for P3 (GPS) time transfer and for E3 (Galileo) time transfer within the given combined uncertainties.

9.1. GPS delays.

Table 19 provides the final results of the calibration campaign for GPS delays for all involved stations. Table 20 provides the conservative $k = 2$ expanded uncertainties for all GPS codes in line with EURAMET requirements.

Table 19. Summary of GPS calibrations on the calibration trip (all values in ns).

BIPM code	RINEX name	Cal Id	Date	$u_{\text{CAL}}(\text{P3})$	INTDLY P1	INTDLY P2
Reference system						
OP73	OP7300FRA	1001-2020	2021	1.5 [*]	29.5	26.3
Visited systems						
LU01	LU0100LUX	1014-2023	2023	0.8	28.2	25.6
LU02	LU0200LUX	1014-2023	2023	0.8	30.6	28.3

[*] Conventional combined uncertainty value for G1 laboratories.

Table 20. Conservative $k = 2$ expanded GPS code uncertainties following EURAMET standard (all values in ns).

BIPM code	RINEX name	$u(\text{P1})$	$u(\text{P2})$	$u(\text{P3})$
LU01	LU0100LUX	1.3	1.2	1.6
LU02	LU0200LUX	1.3	1.2	1.6

9.2. Galileo delays.

Table 21 provides the final results of the calibration campaign for Galileo delays for all involved stations. Table 22 provides the conservative $k = 2$ expanded uncertainties for all Galileo codes in line with EURAMET requirements.

Table 21. Summary Galileo calibrations on the calibration trip (all values in ns).

BIPM code	RINEX name	Cal Id	Date	$u_{CAL}(E3)$	INTDLY E1	INTDLY E5a
Reference system						
OP73	OP7300FRA	1001-2020	2021	1.5 [*]	31.7	31.3
Visited systems						
LU01	LU0100LUX	1014-2023	2023	0.7	30.6	30.8
LU02	LU0200LUX	1014-2023	2023	0.7	32.7	31.3

[*] Conventional combined uncertainty value for G1 laboratories.

Table 22. Conservative $k = 2$ expanded Galileo code uncertainties following EURAMET standard (all values in ns).

BIPM code	RINEX name	$u(E1)$	$u(E5a)$	$u(E3)$
LU01	LU0100LUX	1.3	1.3	1.4
LU02	LU0200LUX	1.3	1.3	1.4

9.3. Comparison with former calibrated delays.

Table 23 is showing the direct comparison with former delays which had been calibrated in 2021 by LNE-SYRTE. It can be seen that the maximum offset is about 1.2 ns, which shows a good stability in the station delays over time. In terms of remote time transfer using either GPS P3 or Galileo E3, the maximum offset is 1.0 ns which is largely in line with the conventional combined G1/G2 uncertainty resulting from this calibration.

Table 23. Comparison of calibrated delays between 2023 and 2021 (all values in ns).

Station	LU01						LU02					
	P1	P2	P3	E1	E5a	E3	P1	P2	P3	E1	E5a	E3
2021	28.2	25.0	33.1	29.9	29.6	30.3	31.0	28.3	35.2	32.7	30.7	35.2
2023	28.2	25.6	32.2	30.6	30.8	30.3	30.6	28.3	34.2	32.7	31.3	34.5
2023 - 2021	0.0	0.6	-0.9	0.7	1.2	0.0	-0.4	0.0	1.0	0.0	0.6	-0.7

10. Appendix.

Annex A. BIPM Information Sheets.	24
Annex B. Plots of raw data and TDEV.	32
Annex C. Uncertainty budgets terms.	44

ANNEX A

Implementation of OP traveling stations in visited sites.

A1. Implementation in OP.

Figure A1 is showing the implementation of OP traveling equipment, namely OP72 and OP74 connected to the same antenna cable and antenna, alongside OP73 reference station in LNE-SYRTE in OP at the start and at the end of the campaign.

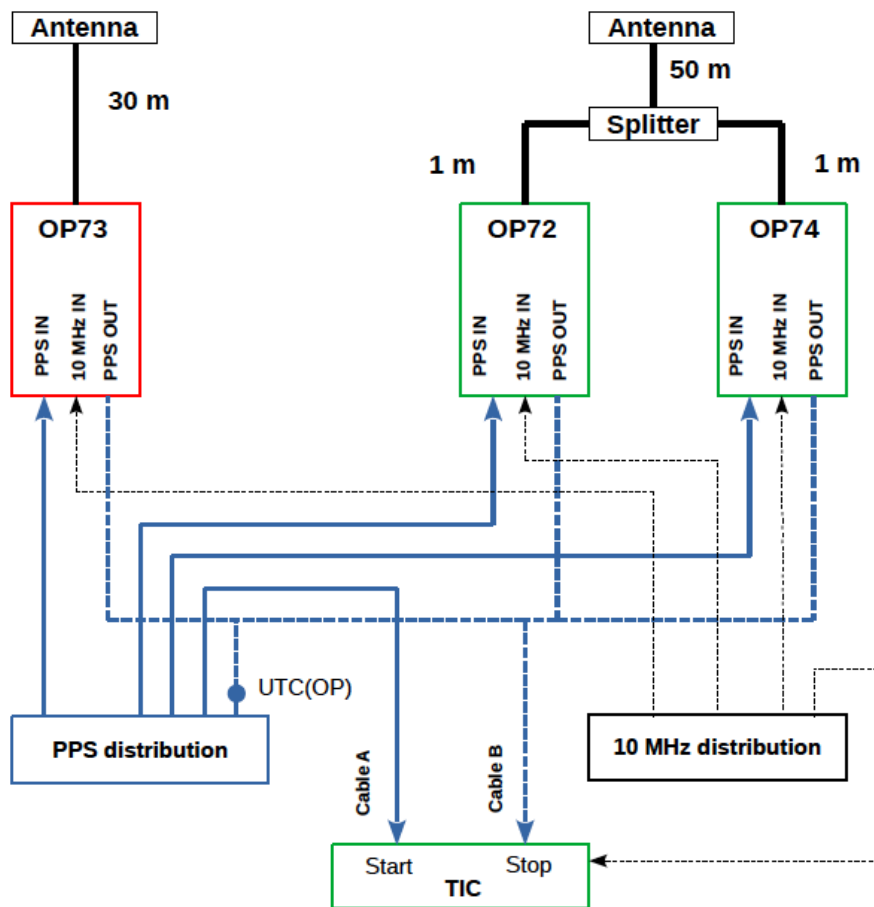


Figure A1. Implementation of OP traveling equipment in OP.

The next pages are providing the BIPM information sheets for OP72 and OP74.

Cal Id: 1014-2023

Version / Date: 19/04/2023

BIPM Information sheet

Laboratory	OP (Open)			
Date and hour beginning of measurements	11 02 2023 00:00			
Date and hour end measurements	16 02 2023 00:00			
Information on the system				
	Local		Traveling	
4-Character BIPM code	OP73	OP72	OP74	
Receiver maker and type	Septentrio PolaRx5TR	Septentrio PolaRx5TR	Septentrio PolaRx5TR	
Receiver serial number	4701467	4701463	4701497	
1 PPS trigger level / V	1 V	1 V	1 V	
Antenna cable marker and type		HY 400 UF	HY 400 UF	
Phase stabilized cable (Y/N)				
Cable length outside building / m	20 m	20 m	20 m	
Antenna maker and type	SEPCHOCKE_B2E6	TWIVP6000	TWIVP6000	
Antenna serial number	5759	33-685000-01-01	33-685000-01-01	
Temperature if stabilized / °C				
Mesured delays / ns				
	Local		Traveling	
Delay from local UTC(k) to receiver 1 PPS_IN				
Delay from 1 PPS_IN to internal reference (see Annex 1)				
Antenna cable delay				
Splitter delay				
Additional cable delay				
Data used for the generation of CCGTIS files				
	Local		Traveling	
INT DLY (GPS) / ns	P1: 29.5	P2: 26.3	P1: 0	P2: 0
INT DLY (Galileo) / ns	E1: 81.7	E5a: 81.3	E1: 0	E5a: 0
CAB DLY / ns	129.6			
REF DLY / ns	85.2	93.408	111.400	
Coordinate reference frame	ITRF	ITRF	ITRF	
Latitude or X / m	4202777.071	4202781.470	4202781.470	
Longitude or Y / m	171367.028	171369.360	171369.360	
Height or Z / m	4778661.392	4778659.104	4778659.104	
General Information				
Rise time of local UTC pulse	< 1 ns			
Air conditioning (Y/N)	Y			
Set temperature value and uncertainty	22°C +/- 1°C			
Set humidity value and uncertainty	22°C +/- 1°C			

Cal Id: 1014-2023

Version / Date: 19/04/2023

BIPM Information sheet

Laboratory	OP (Close)		
Date and hour beginning of measurements	22 03 2023 00:00		
Date and hour end measurements	27 03 2023 00:00		
Information on the system			
	Local	Traveling	
4-Character BIPM code	OP73	OP72	OP74
Receiver maker and type	Septentrio PolaRx5TR	Septentrio PolaRx5TR	Septentrio PolaRx5TR
Receiver serial number	4701467	4701463	4701497
1 PPS trigger level / V	1 V	1 V	1 V
Antenna cable marker and type		HY 400 UF	HY 400 UF
Phase stabilized cable (Y/N)			
Cable length outside building / m	20 m	20 m	20 m
Antenna maker and type	SEPCHOKE_B2E6	TWIVP6000	TWIVP6000
Antenna serial number	5759	33-685000-01-01	33-685000-01-01
Temperature if stabilized / °C			
Mesured delays / ns			
	Local	Traveling	
Delay from local UTC(k) to receiver 1 PPS_IN			
Delay from 1 PPS_IN to internal reference (see Annex 1)			
Antenna cable delay			
Splitter delay			
Additional cable delay			
Data used for the generation of CCGTIS files			
	Local	Traveling	
INT DLY (GPS) / ns	P1: 29.5 P2: 26.3	P1: 0 P2: 0	P1: 0 P2: 0
INT DLY (Galileo) / ns	E1: 31.7 E5a: 31.3	E1: 0 E5a: 0	E1: 0 E5a: 0
CAB DLY / ns	129.6		
REF DLY / ns	85.2	93.350	111.372
Coordinate reference frame	ITRF	ITRF	ITRF
Latitude or X / m	4202777.071	4202781.456	4202781.456
Longitude or Y / m	171367.028	171369.346	171369.346
Height or Z / m	4778661.392	4778659.090	4778659.090
General Information			
Rise time of local UTC pulse	< 1 ns		
Air conditioning (Y/N)	Y		
Set temperature value and uncertainty	22°C +/- 1°C		
Set humidity value and uncertainty	22°C +/- 1°C		

A2. Implementation in ILNAS.

The next pages are providing the BIPM information sheets for each ILNAS station.

Cal Id: 1014-2023

Version / Date: 2023-04-14

BIPM Infomtion sheet

Laboratory	LUX			
Date and hour beginning of measurements	60004,500000			
Date and hour end measurements	60016,500000			
Information on the system				
	Local		Traveling	
4-Character BIPM code	LU01	OP72	OP74	
Receiver maker and type	Septentrio PolaRx5TR	Septentrio PolaRx5TR	Septentrio PolaRx5TR	
Receiver serial number	4701202			
1 PPS trigger level / V	1	1	1	
Antenna cable marker and type	H+S Spuma 400			
Phase stabilized cable (Y/N)	N			
Cable length outside building / m	< 2 m			
Antenna maker and type	SEPCHOKE B3E6 SPK			
Antenna serial number	5151			
Temperature if stabilized / °C	na			
Measured delays / ns				
	Local		Traveling	
Delay from local UTC(k) to receiver 1 PPS_IN	36,57	50,17	68,24	
Delay from 1 PPS_IN to internal reference (see Annex 1)	34,52	38,05	56,12	
Antenna cable delay	117,4			
Splitter delay	na			
Additional cable delay	na			
Data used for the generation of CGGTTS files				
	Local		Traveling	
INT DLY (GPS) / ns	P1: <input type="text"/> P2: <input type="text"/>	P1: <input type="text"/> P2: <input type="text"/>	P1: <input type="text"/> P2: <input type="text"/>	
INT DLY (Galileo) / ns	E1: <input type="text"/> E5a: <input type="text"/>	E1: <input type="text"/> E5a: <input type="text"/>	E1: <input type="text"/> E5a: <input type="text"/>	
CAB DLY / ns	<input type="text"/>	<input type="text"/>	<input type="text"/>	
REF DLY / ns	<input type="text"/>	<input type="text"/>	<input type="text"/>	
Coordinate reference frame	<input type="text"/>	<input type="text"/>	<input type="text"/>	
Latitude or X / m	<input type="text"/>	<input type="text"/>	<input type="text"/>	
Longitude or Y / m	<input type="text"/>	<input type="text"/>	<input type="text"/>	
Height or Z / m	<input type="text"/>	<input type="text"/>	<input type="text"/>	
General Information				
Rise time of local UTC pulse	350 ps			
Air conditioning (Y/N)	Y			
Set temperature value and uncertainty	23 °C +/- 3 °C < 80 HR			
Set humidity value and uncertainty	23 °C +/- 3 °C < 80 HR			

Cal Id: 1014-2023

Version / Date: 2023-04-14

BIPM Infortion sheet

Laboratory	LUX					
Date and hour beginning of measurements	60004.500000					
Date and hour end measurements	60016.500000					
Information on the system						
	Local			Traveling		
4-Character BIPM code	LU02	OP72	OP74			
Receiver maker and type	Septentrio PolaRx5TR	Septentrio PolaRx5TR	Septentrio PolaRx5TR			
Receiver serial number	4701382					
1 PPS trigger level / V	1.0	1	1			
Antenna cable marker and type	H+S Spuma 400					
Phase stabilized cable (Y/N)	N					
Cable length outside building / m	< 2 m					
Antenna maker and type	SEPCHOKE B3E6 SPK					
Antenna serial number	5668					
Temperature if stabilized / °C	na					
Mesured delays / ns						
	Local			Traveling		
Delay from local UTC(k) to receiver 1 PPS_IN	38.61	50.17	68.24			
Delay from 1 PPS_IN to internal reference (see Annex 1)	37.07	38.05	56.12			
Antenna cable delay	160.63					
Splitter delay	na					
Additional cable delay	na					
Data used for the generation of CGGTIS files						
	Local			Traveling		
INT DLY (GPS) / ns	P1:	P2:	P1:	P2:	P1:	P2:
INT DLY (Galileo) / ns	E1:	E5a:	E1:	E5a:	E1:	E5a:
CAB DLY / ns						
REF DLY / ns						
Coordinate reference frame						
Latitude or X / m						
Longitude or Y / m						
Height or Z / m						
General Information						
Rise time of local UTC pulse	350 ps					
Air conditioning (Y/N)	Y					
Set temperature value and uncertainty	23 °C +/- 3 °C <80 %HR					
Set humidity value and uncertainty	23 °C +/- 3 °C <80 %HR					

ANNEX B**Raw data and TDEV.**

- | | |
|--|----|
| 1. Reminder of equipment and planning. | B2 |
| 2. GPS calibration of OP72 and OP74 against OP73. | B2 |
| 2.1. Results of raw data processing. | |
| 2.2. Plots of raw data and TDEV. | |
| 3. GPS calibration of visited stations. | B4 |
| 4.1. Results of raw data processing. | |
| 4.2. Plots of raw data and TDEV. | |
| 4. Galileo calibration of OP72 and OP74 against OP73. | B6 |
| 3.1. Results of raw data processing. | |
| 3.2. Plots of raw data and TDEV. | |
| 5. Galileo calibration of visited stations. | B9 |
| 5.1. Results of raw data processing. | |
| 5.2. Plots of raw data and TDEV. | |

1. Reminder of equipment and planning.

Institute	Equipment status	MJD of measurement	Receiver type	BIPM code	RINEX name
OP	Traveling	59986 - 60030	Septentrio PolaRx5TR	OP72	OP72
OP	Traveling	59986 - 60030	Septentrio PolaRx5TR	OP74	OP74
OP	G1 reference	59986 - 60030	Septentrio PolaRx5TR	OP73	OP7300FRA
ILNAS	G2	60005-60015	Septentrio PolaRx5TR	LU01	LU0100LUX
ILNAS	G2	60005-60015	Septentrio PolaRx5TR	LU02	LU0200LUX

2. GPS calibration of OP72 and OP74 against OP73.

2.1. Results of raw data processing.

Pair	MJD of measurement	RawDiff P1	TDEV	RawDiff P2	TDEV
OP72 - OP73	59986-59991	- 57.227	0.027	- 58.517	0.030
OP74 - OP73	59986-59991	- 39.904	0.021	- 41.285	0.024
OP72 - OP73	60025-60030	- 57.063	0.031	- 58.526	0.027
OP74 - OP73	60025-60030	- 39.774	0.031	- 41.297	0.026

2.2. Plots of raw data and TDEV.

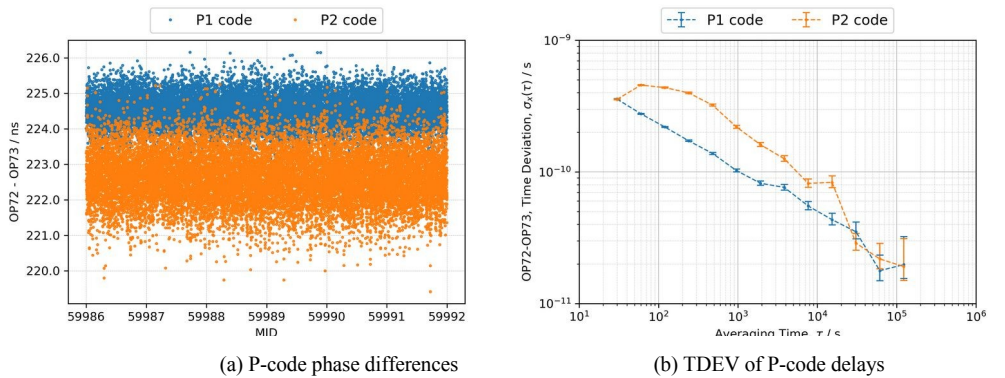


Figure B1: GPS relative calibration of OP72 with respect to OP73 (start).

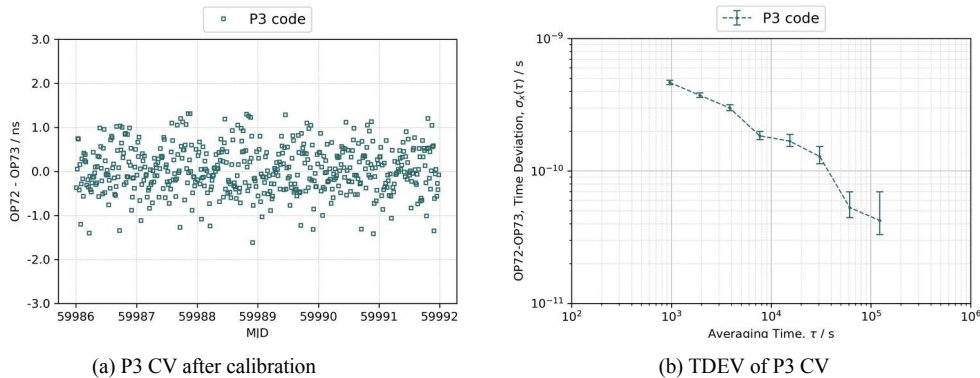


Figure B2: P3 CV time difference of OP72 with respect to OP73 (start).

B2

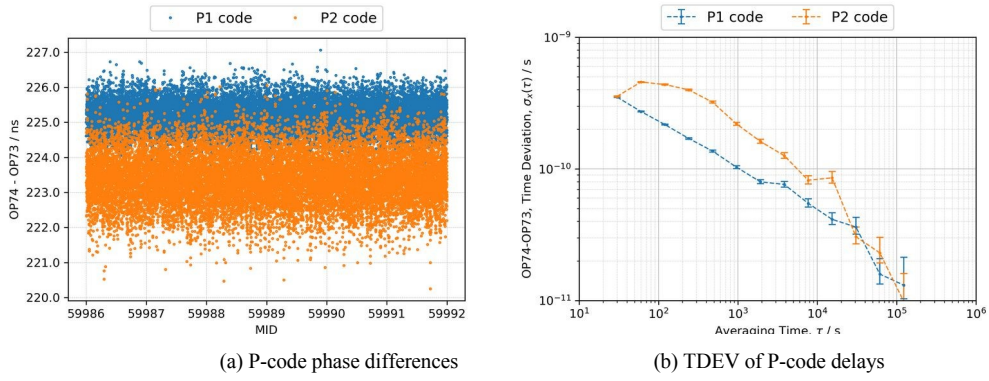


Figure B3: GPS relative calibration of OP74 with respect to OP73 (start).

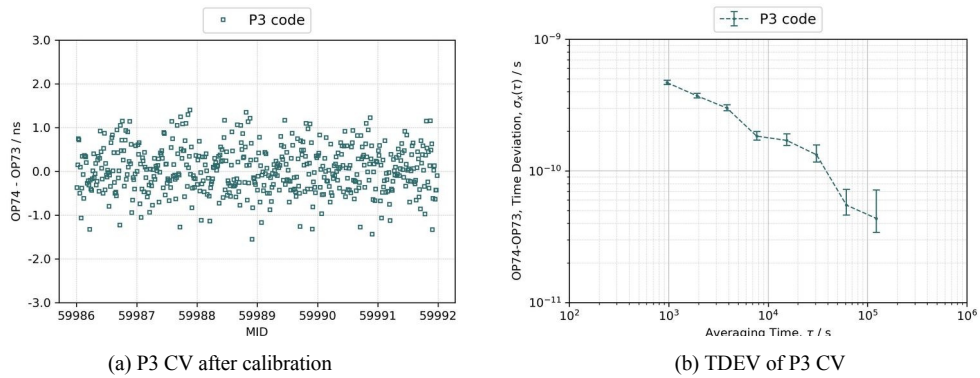


Figure B4: P3 CV time difference of OP74 with respect to OP73 (start).

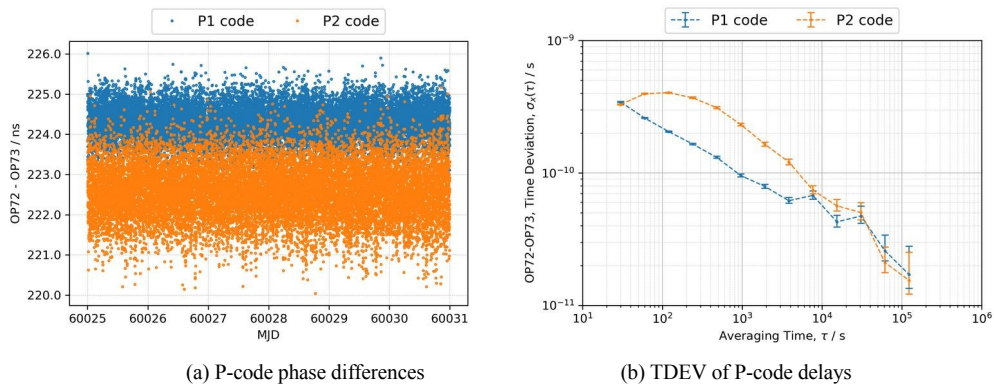


Figure B5: GPS relative calibration of OP72 with respect to OP73 (closure).

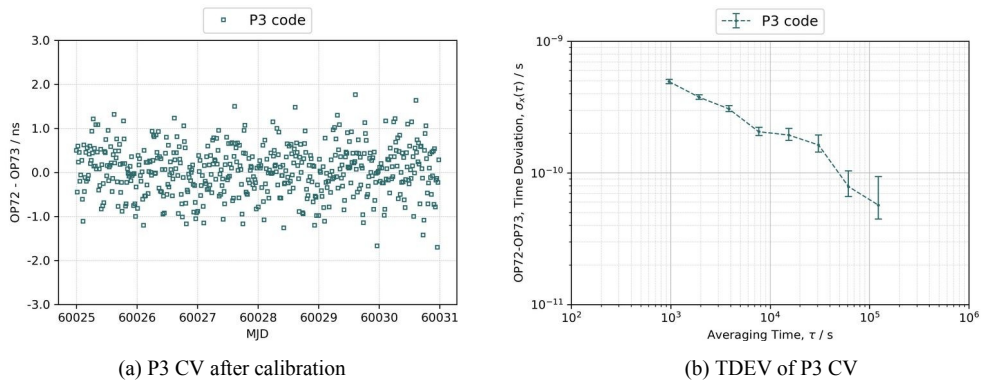


Figure B6: P3 CV time difference of OP72 with respect to OP73 (closure).

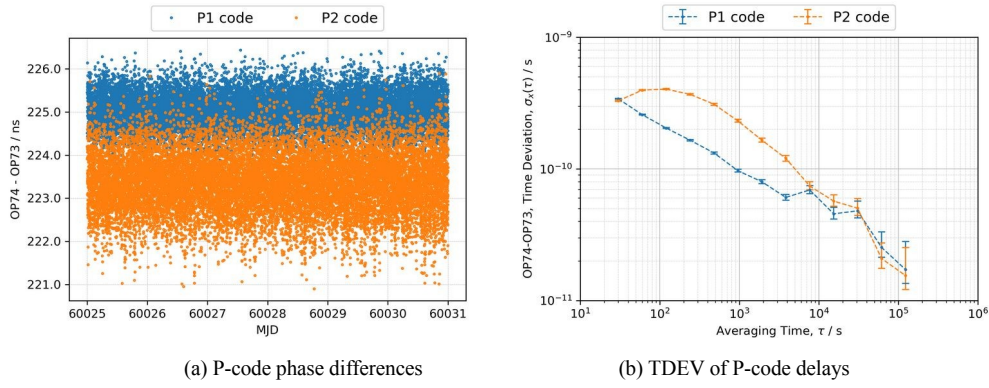


Figure B7: GPS relative calibration of OP74 with respect to OP73 (closure).

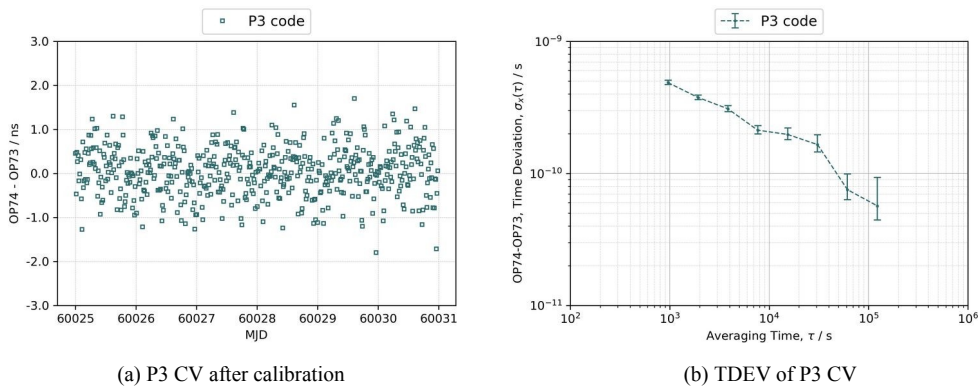


Figure B8: P3 CV time difference of OP74 with respect to OP73 (closure).

3. GPS calibration of visited stations against OP72 and OP74.

3.1. Results of raw data processing.

Pair	MJD of measurement	RawDiff P1	TDEV	RawDiff P2	TDEV
LU01 - OP72	60005-60015	65.255	0.091	66.023	0.051
LU01 - OP74	60005-60015	47.796	0.090	48.621	0.051
LU02 - OP72	60005-60015	21.763	0.090	22.187	0.049
LU02 - OP74	60005-60015	4.303	0.091	4.786	0.050

3.2. Plots of raw data and TDEV.

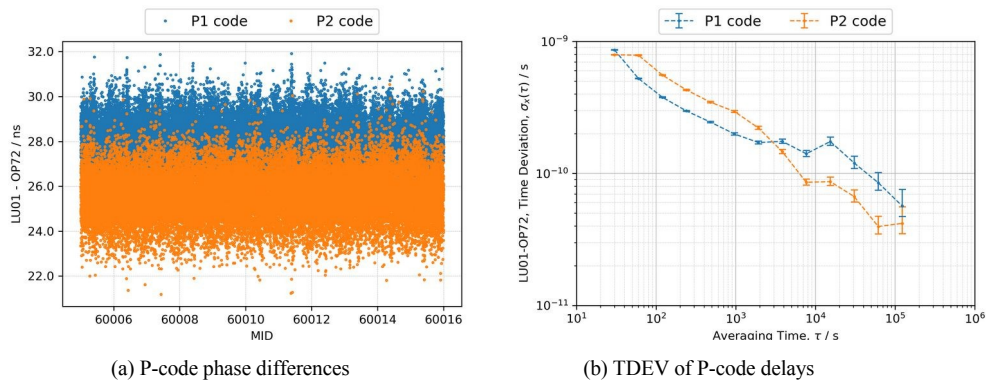
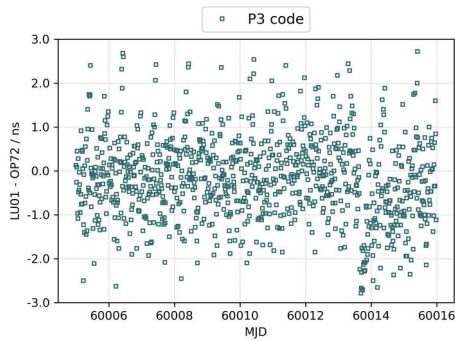
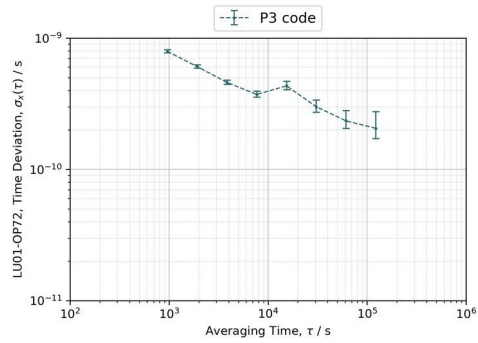


Figure B9: GPS relative calibration of LU01 with respect to OP72.

B4

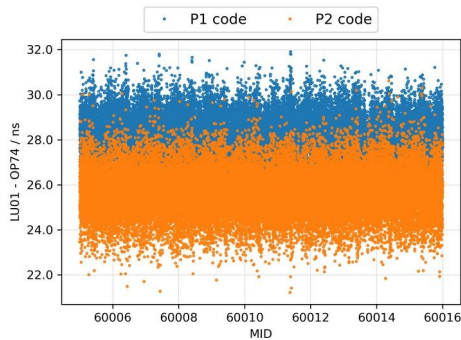


(a) P3 CV after calibration

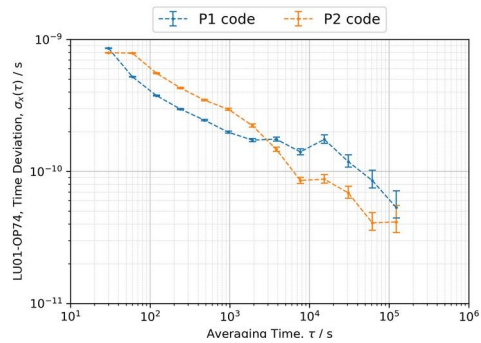


(b) TDEV of P3 CV

Figure B10: P3 CV time difference of LU01 with respect to OP72.

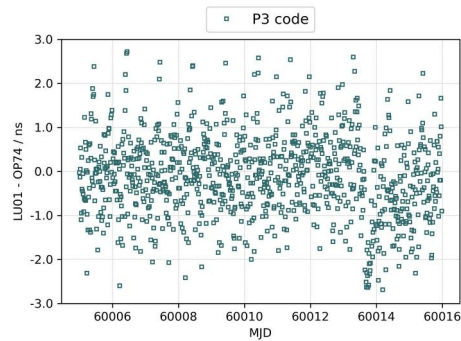


(a) P-code phase differences

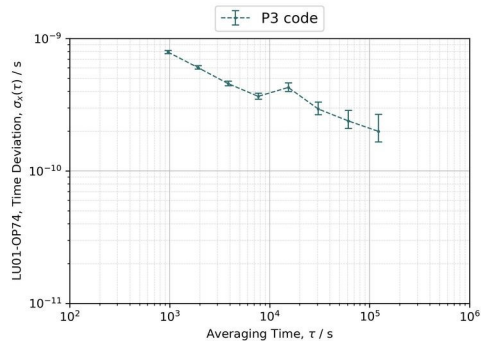


(b) TDEV of P-code delays

Figure B11: GPS relative calibration of LU01 with respect to OP74.

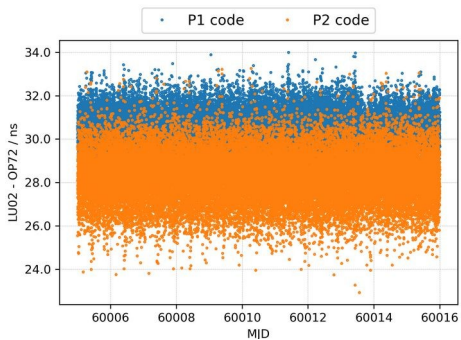


(a) P3 CV after calibration

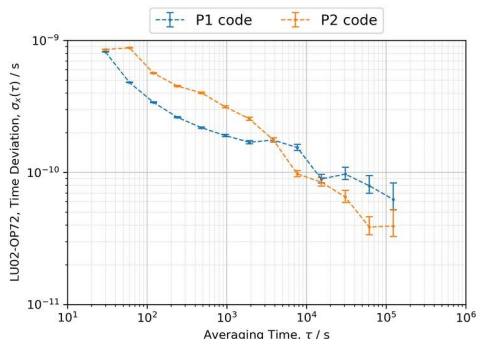


(b) TDEV of P3 CV

Figure B12: P3 CV time difference of LU01 with respect to OP74.



(a) P-code phase differences



(b) TDEV of P-code delays

Figure B13: GPS relative calibration of LU02 with respect to OP72.

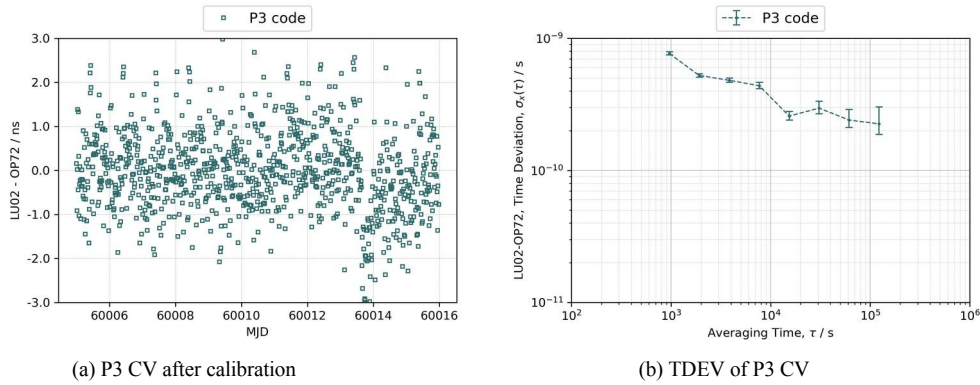


Figure B14: P3 CV time difference of LU02 with respect to OP72.

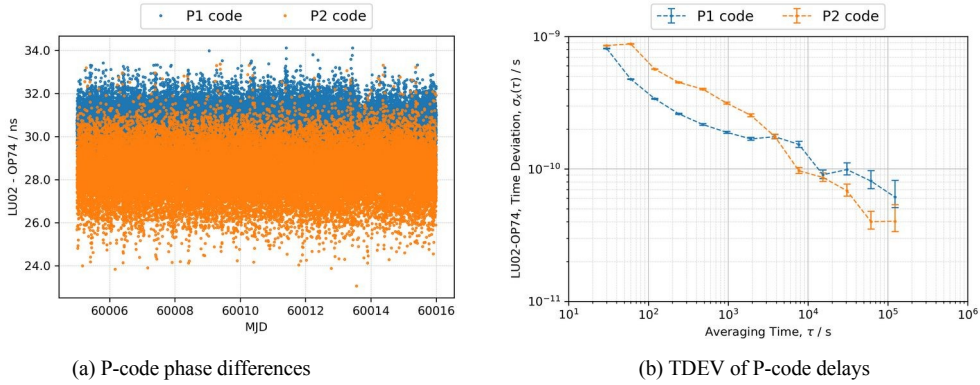


Figure B15: GPS relative calibration of LU02 with respect to OP74.

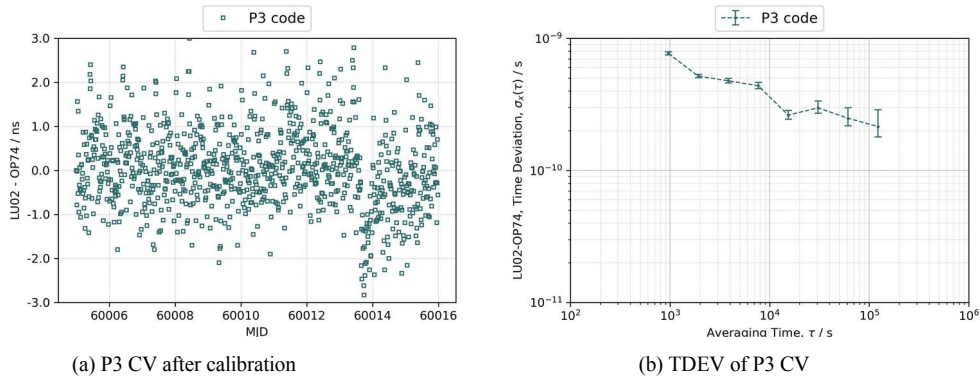


Figure B16: P3 CV time difference of LU02 with respect to OP74.

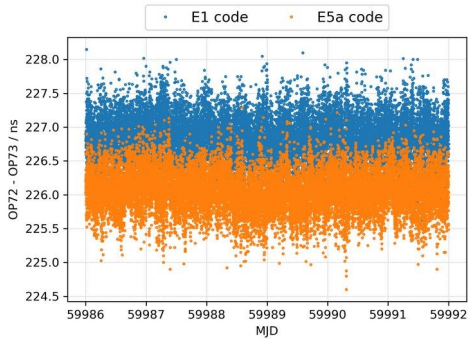
4. Galileo calibration of OP72 and OP74 with respect to OP73.

4.1. Results of raw data processing.

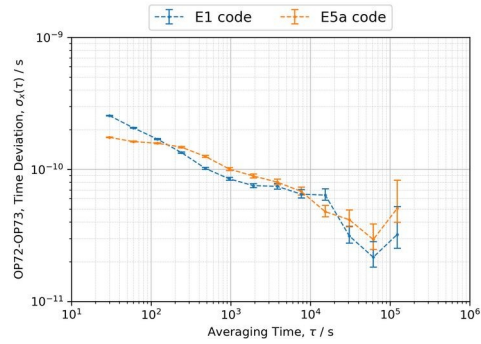
Pair	MJD of measurement	RawDiff E1	TDEV	RawDiff E5a	TDEV
OP72 – OP73	59986-59991	- 57.332	0.038	- 56.947	0.057
OP74 – OP73	59986-59991	- 40.149	0.034	- 39.701	0.043
OP72 – OP73	60025-60030	- 57.148	0.046	- 56.935	0.045
OP74 – OP73	60025-60030	- 40.004	0.048	- 39.690	0.046

4.2 Plots of raw data and TDEV.

B6

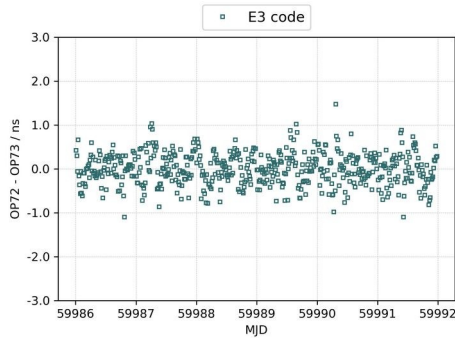


(a) E-code phase differences

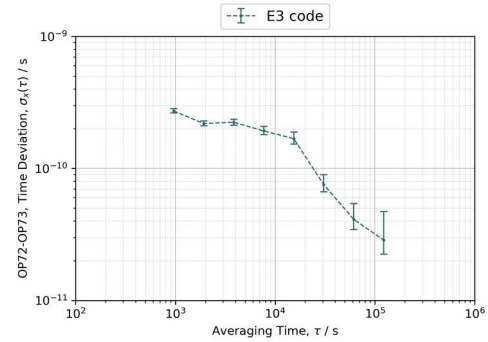


(b) TDEV of E-code delays

Figure B17: Galileo relative calibration of OP72 with respect to OP73 (start).

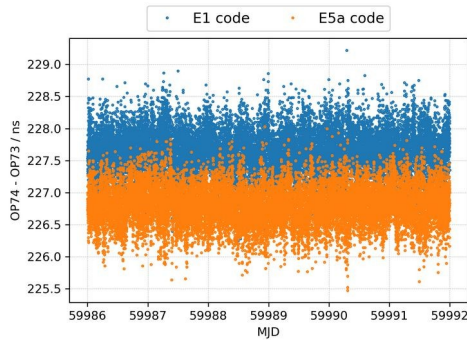


(a) E3 CV after calibration

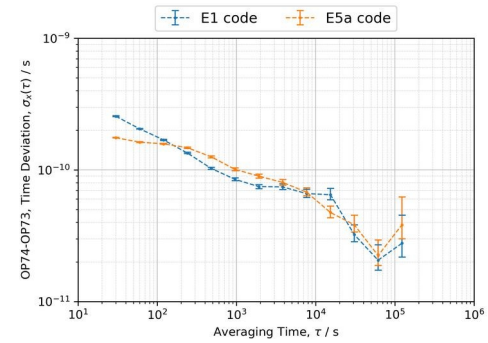


(b) TDEV of E3 CV

Figure B18: E3 CV time difference of OP72 with respect to OP73 (start).

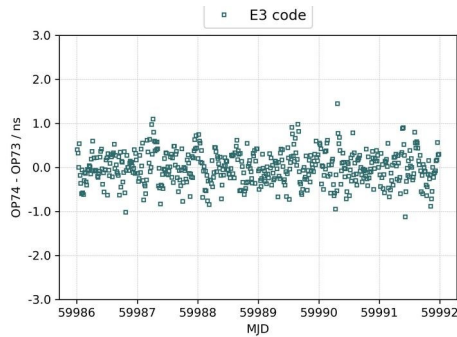


(a) E-code phase differences

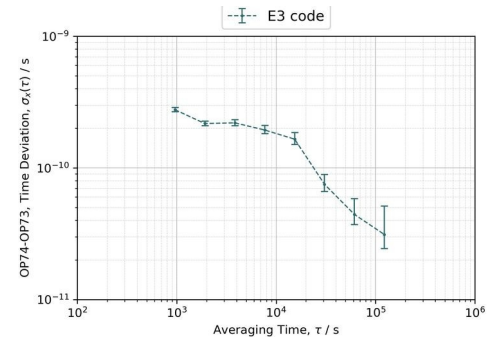


(b) TDEV of E-code delays

Figure B19: Galileo relative calibration of OP74 with respect to OP73 (start).

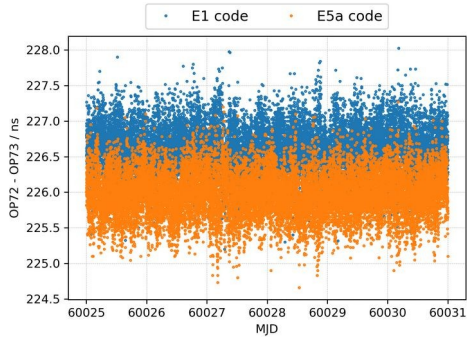


(a) E3 CV after calibration

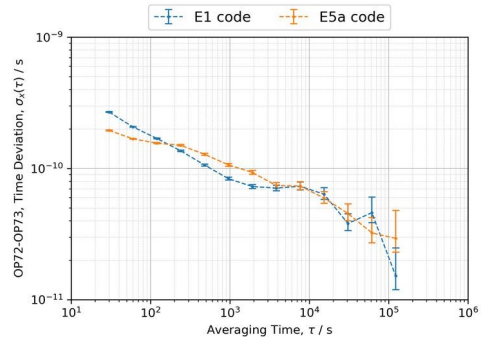


(b) TDEV of E3 CV

Figure B20: E3 CV time difference of OP74 with respect to OP73 (start).

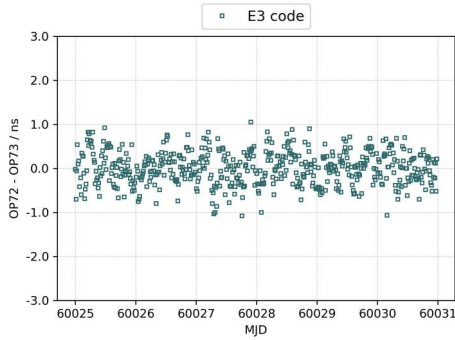


(a) E-code phase differences

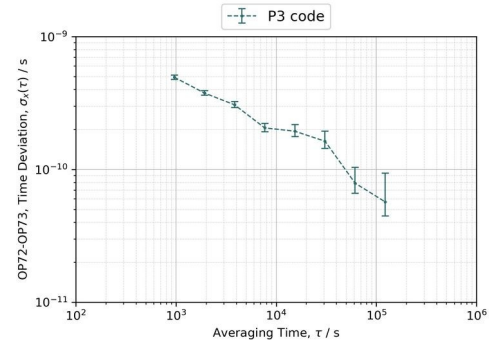


(b) TDEV of E-code delays

Figure B21: Galileo relative calibration of OP72 with respect to OP73 (closure).

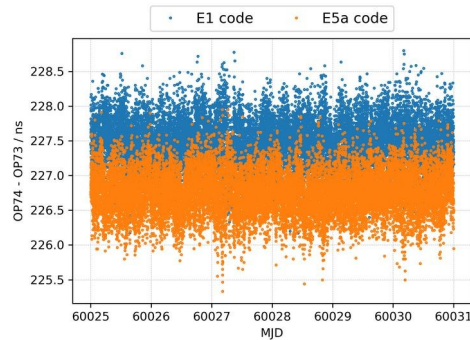


(a) E3 CV after calibration

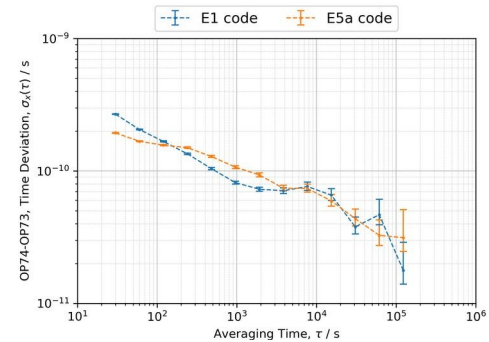


(b) TDEV of E3 CV

Figure B22: E3 CV time difference of OP72 with respect to OP73 (closure).

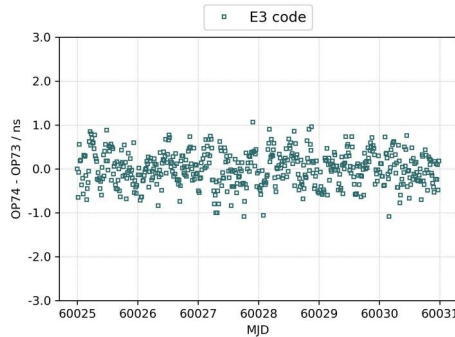


(a) E-code phase differences

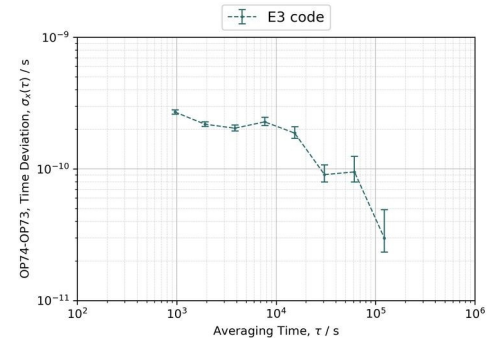


(b) TDEV of E-code delays

Figure B23: Galileo relative calibration of OP74 with respect to OP73 (closure).



(a) E3 CV after calibration



(b) TDEV of E3 CV

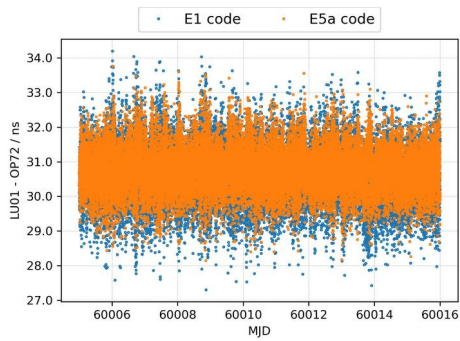
Figure B24: E3 CV time difference of OP74 with respect to OP73 (closure).

5. Galileo calibration of visited stations against OP72 and OP74.

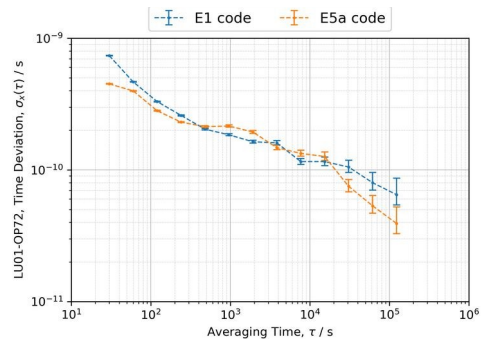
5.1. Results of raw data processing.

Pair	MJD of measurement	RawDiff E1	TDEV	RawDiff E5a	TDEV
LU01 - OP72	60005-60015	65.130	0.092	64.270	0.059
LU01 - OP74	60005-60015	47.815	0.091	46.852	0.063
LU02 - OP72	60005-60015	21.881	0.104	22.595	0.060
LU02 - OP74	60005-60015	4.566	0.103	5.178	0.060

5.2. Plots of raw data and TDEV.

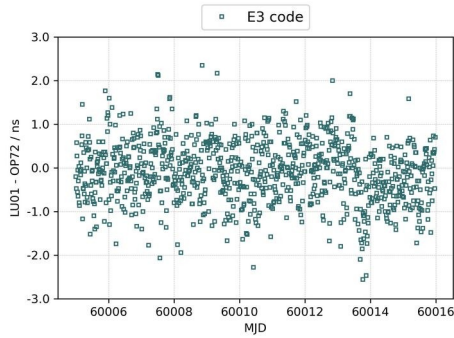


(a) E-code phase differences

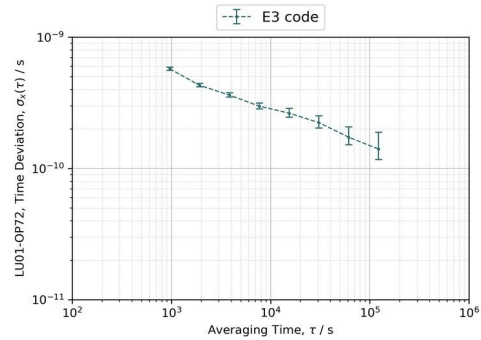


(b) TDEV of E-code delays

Figure B25: Galileo relative calibration of LU01 with respect to OP72.

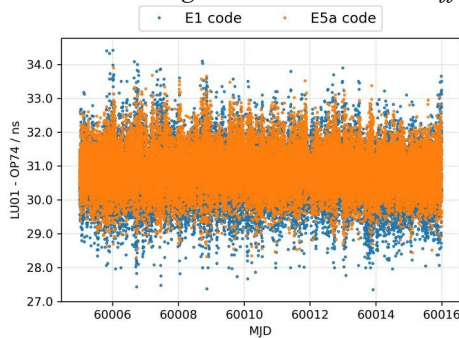


(a) E3 CV after calibration

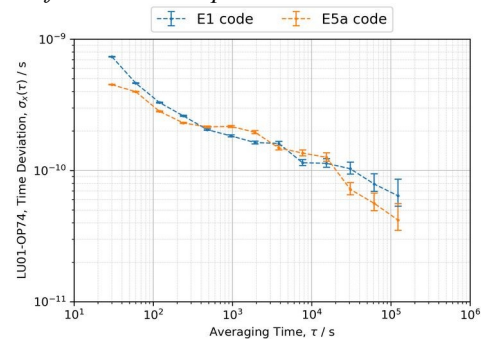


(b) TDEV of E3 CV

Figure B26: E3 CV time difference of LU01 with respect to OP72.

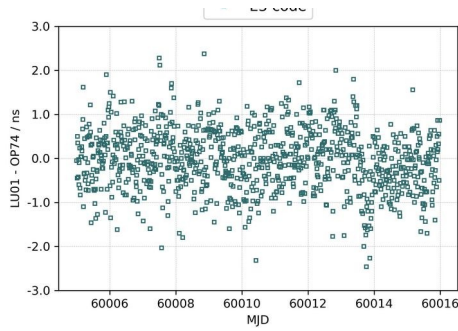


(a) E-code phase differences

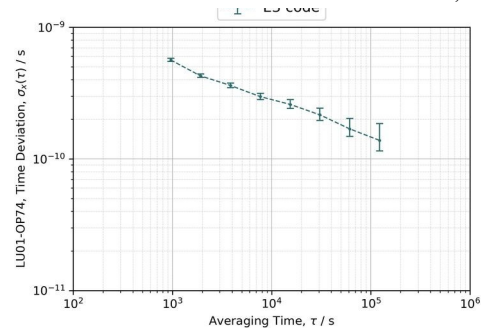


(b) TDEV of E-code delays

Figure B27: Galileo relative calibration of LU01 with respect to OP74.

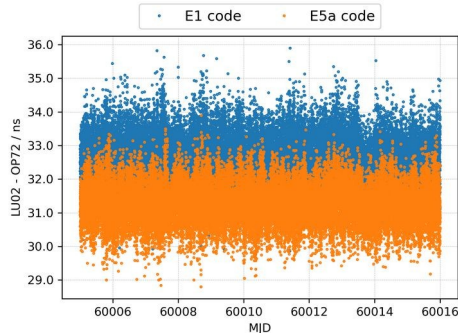


(a) E3 CV after calibration

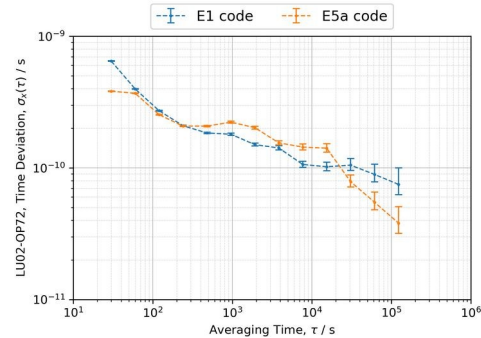


(b) TDEV of E3 CV

Figure B28: E3 CV time difference of LU01 with respect to OP74.

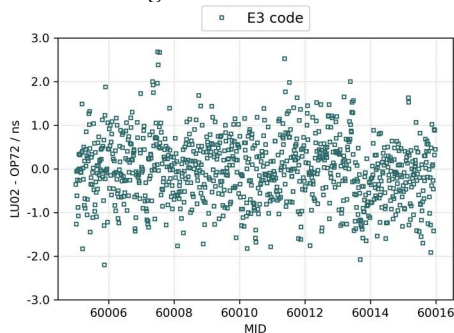


(a) E-code phase differences

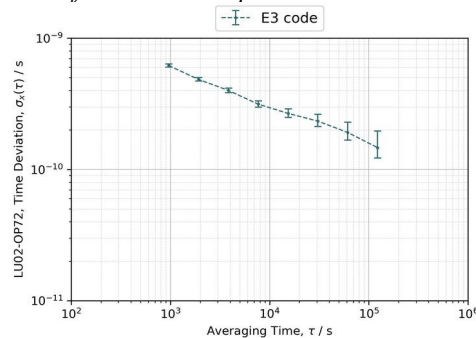


(b) TDEV of E-code delays

Figure B29: Galileo relative calibration of LU02 with respect to OP72.

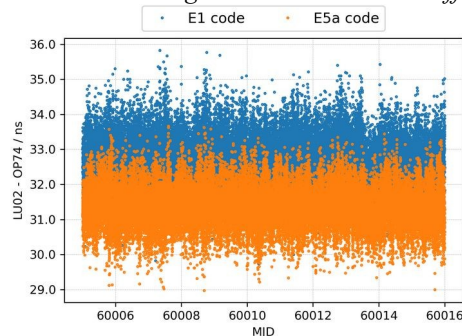


(a) E3 CV after calibration

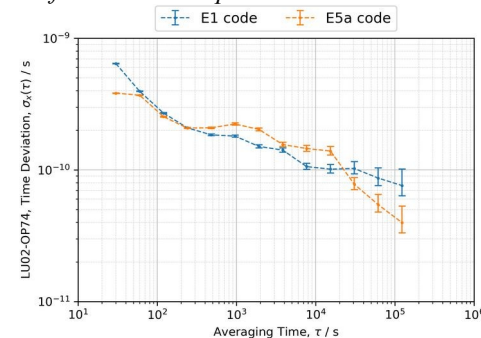


(b) TDEV of E3 CV

Figure B30: E3 CV time difference of LU02 with respect to OP72.

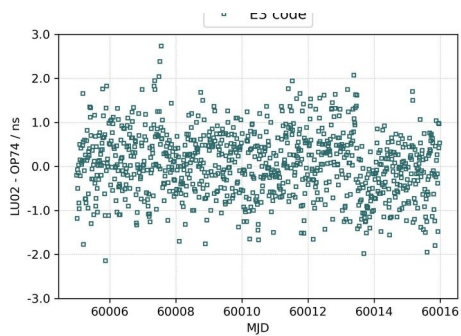


(a) E-code phase differences

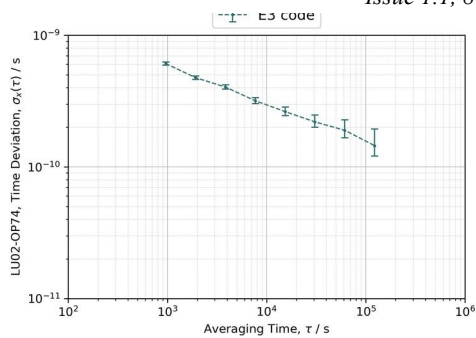


(b) TDEV of E-code delays

Figure B31: Galileo relative calibration of LU02 with respect to OP74.



(a) E3 CV after calibration



(b) TDEV of E3 CV

Figure B32: E3 CV time difference of LU02 with respect to OP74.

ANNEX C

Uncertainty budget terms.

1. Type A uncertainty.

The statistical uncertainty $u_a(A-B)$ for the comparison between two GNSS stations A and B and for each GNSS code is evaluated by computing the upper limit of the error bar of the TDEV at 1 d when possible, or otherwise the upper limit of the last error bar available. The sampling periods of computed calibrated offset usually lead to TDEV data available for 61 440 s and 122 880 s averaging periods. The computed u_a is obtained by a linear interpolation between consecutive TDEV data at an 86 400 s averaging period. When required, a simple quadratic sum leads to the Type A uncertainty required for an uncertainty budget computation.

2. Type B uncertainty.

Here are the u_b uncertainties taken into account in the uncertainty budget computations, together with the way they are estimated when necessary.

- $u_{b,1}$ observed maximum misclosure. This uncertainty component is an estimation of the stability of the traveling equipment during the campaign. The misclosure $u_{b,1}$ we used here is the actual misclosure between the start and the end of the campaign..
- $u_{b,11}$ position error at reference site. The position of the center of phase of traveling antenna is estimated at opening and closure by using the NRCAN PPP software, while for the OP reference station antenna the coordinates of the last G1 calibration are used. Note that this computation is achieved by using GPS data only. This might lead to a small bias on the phase center of the antenna for Galileo signals. We safely choose a conventional value of 200 ps (≈ 6 cm) for the position error at the reference site.
- $u_{b,12}$ position error at visited site. At visited sites the position of the center of phase of all antennas is estimated by using the NRCAN PPP software. Note that this computation is achieved by using GPS data only. This might lead to a small bias on the phase center of the antenna for Galileo signals. We safely choose a conventional value of 200 ps (≈ 6 cm) for the position error at all visited sites.
- $u_{b,13}$ multipath at reference site. We assume in all cases a conventional value of 200 ps, which is in line with some experiment achieved at OP and ORB, especially when using the calibration software developed at OP, where outliers are properly averaged out. (see: G.D. Rovera, M. Abgrall, P. Urich, P. Defraigne and B. Bertrand, “GNSS antenna multipath effects”, Proc. of the 31st European Frequency and Time Forum (EFTF), Torino, 2018).
- $u_{b,14}$ multipath at visited site. Same as above.
- $u_{b,21}$ REF DLY (traveling receiver at reference lab). Uncertainty of the measure of the time difference between the reference point of the traveling receiver and the local UTC(k). The used value is the quadratic sum of an uncertainty value attributed to the Time Interval Counter (TIC) with the standard deviation of the actual measurement. When the REF DLY is obtained by summing several individual measurement the uncertainty is increased by quadratic sum as required. We use 220 ps as conservative conventional value.
- $u_{b,22}$ REF DLY (traveling receiver at visited lab). Same as above. This is possible because the TIC we are using for all REF DLY measurements is traveling along with the OP GNSS stations.

- $u_{b,TOT}$: Quadratic sum of all previous u_b .
- $u_{b,31}$ REFDFLY uncertainty of the GNSS reference station to its local UTC(k). Computed similarly as $u_{b,21}$. This term can be set to 0 when the GNSS reference station has been recently calibrated, the uncertainty of REFDFLY being already included in the conventional uncertainty decided by the CCTF WG on GNSS.
- $u_{b,32}$ REFDFLY uncertainty (at visited lab) of the link of the visited station to its local UTC(k). Computed similarly as $u_{b,21}$. When this delay is measured and the $u_{b,32}$ is taken into account, the local distribution system can be modified afterwards without losing the calibration of the local GNSS station, provided the new REFDFLY is taken into account afterwards
- $u_{b,41}$ uncertainty of the antenna cable delay at reference station. The chosen value here is based on a comprehensive study which is available in reference [4].
- $u_{b,42}$ uncertainty of antenna cable delay at visited station. Same as just above. When for some reason the antenna cable of the traveling system is changed during the campaign, $u_{b,42}$ is typically obtained from the quadratic sum of the uncertainty of the antenna cable delay actually used at the visited station and the uncertainty of the antenna cable delay of the traveling equipment.
- $u_{b,SYS}$: Quadratic sum of all type B uncertainties above.

3. Combined uncertainty.

- u_{CAL0} : Quadratic sum of u_a and $u_{b,SYS}$. This uncertainty is for the link between the calibrated station and the reference station, without taking into account the uncertainty of this reference station.

Note finally that, in our computation, P3 uncertainty values are not based on a linear combination of P1 and P2 uncertainty values but estimated in a similar way as for P1 and P2. And this is also the case for E3 uncertainty values, which are computed in a similar way as E1 and E5a uncertainty values.

END OF DOCUMENT